Pergamon

Bioorganic & Medicinal Chemistry 7 (1999) 2499–2507

BIOORGANIC & MEDICINAL CHEMISTRY

Cross-Linking of Proteins by Maillard Processes: Characterization and Detection of Lysine–Arginine Cross-Links Derived from Glyoxal and Methylglyoxal

Markus O. Lederer* and Ralph G. Klaiber

Institut für Lebensmittelchemie (170), Universität Hohenheim, Garbenstr. 28, D-70593 Stuttgart, Germany

Received 3 March 1999; accepted 7 June 1999

Abstract—α-Dicarbonyl compounds, such as glyoxal and methylglyoxal, are crucial intermediates in the browning and cross-linking of proteins by reducing sugars in the course of the Maillard reaction. The cross-linking units 2-ammonio-6-({2-[(4-ammonio-5-oxido-5-oxopentyl)amino]-4,5-dihydro-1*H*-imidazol-5-ylidene}amino)hexanoate (**9**) and 2-ammonio-6-({2-[(4-ammonio-5-oxido-5-oxopentyl) amino]-4-methyl-4,5-dihydro-1*H*-imidazol-5-ylidene}amino)hexanoate (**10**), designated as GODIC and MODIC, are identified and quantified from glyoxal/methylglyoxal-bovine serum albumin (BSA) incubations. Independent syntheses and unequivocal structural characterization are given for **9** and **10**. A protocol was established for their determination by liquid chromatography–mass spectrometry (LC–MS) with electrospray ionization (ESI). BSA and the respective α-dicarbonyl compound were incubated at 37°C, pH 7.4 for 1 week, and the time-dependent formation of **9** and **10** was observed. The maximum value obtained from a solution containing 50 g/L BSA and 2 mM glyoxal or methylglyoxal after a 7-day incubation period corresponds to an arginine derivatization quota of 13.0 ± 0.32 mmol **9**/mol Arg or 3.0 ± 0.12 mmol **10**/mol Arg. The cross-links **9** and **10** were also detected in a D-glucose–BSA incubation. From these results, it seems justified to assign an important role to **9** and **10** in the cross-linking of proteins in vivo as well as in foodstuffs. In an additional model study, formation of **9** and **10** was compared to that of the imidazolium cross-links GOLD **3** and MOLD **4**.

Introduction

The Maillard reaction or 'nonenzymatic browning' is a complex series of reactions between reducing carbohydrates with lysine side chains and N-terminal amino groups of proteins. This process initially leads to rather labile Schiff bases which as a rule rearrange to the more stable Amadori products. The Amadori compounds are slowly degraded, in complex reaction pathways via dicarbonyl intermediates, to a plethora of compounds[1,2] designated summarily as 'advanced glycation end products' (AGEs); this overall reaction sequence proceeds both in vitro and in vivo.[3,4] In long-lived tissue proteins, these chemical modifications accumulate with age and may contribute to pathophysiologies associated with aging and long-term complications of diabetes and atherosclerosis.[1–8]

One major consequence of the advanced Maillard reaction is the formation of covalently cross-linked proteins. Though not much is known about the chemical nature of the cross-linking units, several investigations have indicated sugar-derived dicarbonyl compounds such as 3-deoxyglucosone (3-DG), methylglyoxal (MGO), or glyoxal (GO) to be involved.[9] MGO may be formed in vitro by reverse aldol reaction (e.g. from 3-DG) and in vivo either enzymatically from dihydroxyacetone phosphate by methylglyoxal synthase and other pathways, or non-enzymatically by elimination of phosphate from glyceraldehyde phosphate or dihydroxyacetone phosphate.[10,11] In contrast, generation of GO requires an oxidation process and can proceed via D-glucose autoxidation,[14] oxidative degradation of Amadori products,[17] termed as glycoxidation, or lipid peroxidation.[12]

On the basis of various model reactions, different mechanisms for cross-linking of amino acid side chains in proteins have been discussed.[13–24] In vivo, pentosidine,[25] fluorophore LM-1,[26] crossline,[27] and MOLD **4**[28] (see Fig. 1) have been detected only in very low amount; hence, other structures must be involved in the extensive protein cross-linking in certain mammalian tissues. For a better understanding of the impact that the Maillard reaction has on aging and diabetes, and for developing effective therapeutic methods to prevent AGE accumulation in tissues, it is an absolute prerequisite to definitively

Key words: Maillard reaction; protein cross-linking; glyoxal; methylglyoxal.
* Corresponding author. Tel.: +49-(0)711-459-4095; fax: +49-(0)711-459-4096; e-mail: ledererm@uni-hohenheim.de

0968-0896/99/$ - see front matter
PII: S0968-0896(99)00212-6

establish the chemical nature of the major protein crosslinks derived from this reaction.

We have recently shown that 2-ammonio-6-{2-[(4-ammonio - 5 - oxido - 5 - oxopentyl)amino] - 6,7 - dihydroxy - 4,5,6,7,8,8a-hexahydroimidazo [4,5-*b*] azepin-4-yl}hexanoate (**1**, see Fig. 1) can be detected in substantial amount from D-glucose-bovine serum albumin (BSA) incubations.[29] Formation of cross-link analogues such as 2-acetylamino-5-[(5-butylimino-4-methyl-4,5-dihydro-1*H*-2-imidazolyl)amino] pentanoic acid (**2**) so far has been proven only for model reactions of MGO and butylamine with α-*N*-acetyl-L-arginine or creatine.[30] We have now synthesized the quasihomologous 2-ammonio-6-({2-[(4-ammonio - 5 - oxido - 5 - oxopentyl)amino] - 4,5 - dihydro - 1*H*-imidazol-5-ylidene}amino)hexanoate (**9**; see Fig. 2) and 2-ammonio-6-({2-[(4-ammonio-5-oxido-5-oxopentyl)amino]-4-methyl-4,5-dihydro-1*H*-imidazol-5-ylidene}amino)hexanoate (**10**), and definitely established their presence in GO–BSA or MGO–BSA as well as D-glucose–BSA incubations. The formation of **9** and **10** was followed by in vitro model studies in comparison to the formation of the corresponding imidazolium compounds **3** and **4** which also represent GO or MGO derived cross-links.

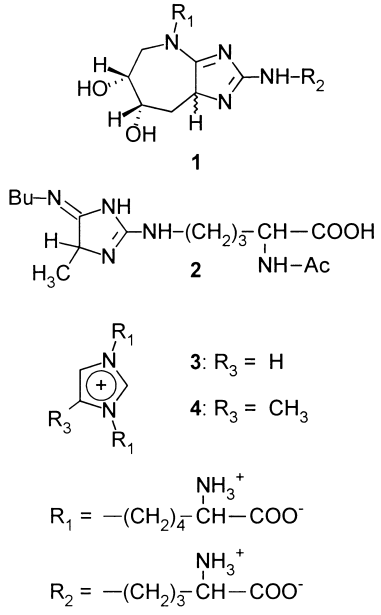

Figure 1. Structural formulae of 2-ammonio-6-{2-[(4-ammonio-5-oxopentyl)amino]-6,7-dihydroxy-4,5,6,7,8,8a-hexahydroimidazo[4,5-*b*] azepin-4-yl}hexanoate (**1**, glucosepan), 2-acetylamino-5-[(5-butylimino-4-methyl-4,5-dihydro-1*H*-2-imidazolyl)amino] pentanoic acid (**2**), 2-ammonio-6-[1-(5-ammonio-6-oxido-6-oxohexyl)imidazolium-3-yl] hexanoate (**3**, GOLD), and 2-ammonio-6-[1-(5-ammonio-6-oxido-6-oxohexyl)-5-methylimidazolium-3-yl] hexanoate (**4**, MOLD).

Results

α-*N*-*t*-BOC-L-Lysine, α-*N*-*t*-BOC-L-arginine, and GO were allowed to react in aqueous phosphate buffer at 50°C under nitrogen atmosphere for 4 days; the respective MGO incubation at 40°C was stopped after 24 h. In each case, the pH was adjusted to 7.4 at the outset of the reaction. The resulting products 2 - [(*tert* - butoxycarbonyl)amino]-6-{[2-({4-[(*tert*-butoxycarbonyl)amino]-5-oxido-5-oxopentyl}amino)-4,5-dihydro-1*H*-imidazol-5-ylidene]amino}hexanoic acid (**7**) and 2 - [(*tert* - butoxycarbonyl)amino]-6-{[2-({4-[(*tert*-butoxycarbonyl)amino]-5-oxido-5-oxopentyl}amino)-4-methyl-4,5-dihydro-1*H*-imidazol-5-ylidene]amino}hexanoic acid (**8**) were identified by high performance liquid chromatography (HPLC) with diode array detection (DAD) since their UV spectra (λ_{max} 242 nm for both) are close to identical to that of **2**.[30] A hypothetical pathway for the formation of **7** and **8** is outlined in Figure 2. Reaction of the aldimines **5** and **6** with the guanidine function of an arginine side chain, followed by H_2O elimination and prototropic rearrangement, leads to compounds **7** and **8**. This reaction sequence is similar to that proposed for the formation of aminoimidazolinone derivatives.[31–33]

HPLC monitoring of preliminary experiments had shown the yield of **7** to increase but slightly with extended incubation time; rather, the abundance of by-products, formed with longer reaction times, severely hampers both work up and purification. Incubation was therefore limited to 4 days. Concentration of **8**, in contrast, reaches a steady state already after 24 h, and remains nearly constant for several days. The assignment of the

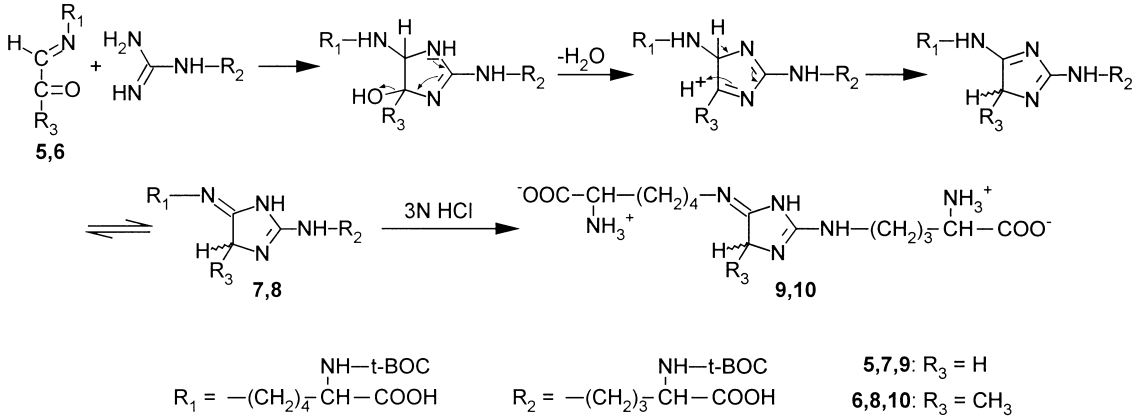

Figure 2. Proposed reaction pathway for the formation of 2-[(*tert*-butoxycarbonyl)amino]-6-{[2-({4-[(*tert*-butoxycarbonyl)amino]-5-oxido-5-oxopentyl}amino)-4,5-dihydro-1*H*-imidazol-5-ylidene]amino}hexanoic acid (**7**) and 2-[(*tert*-butoxycarbonyl)amino]-6-{[2-({4-[(*tert*-butoxycarbonyl)amino]-5-oxido-5-oxopentyl}amino)-4-methyl-4,5-dihydro-1*H*-imidazol-5-ylidene]amino}hexanoic acid (**8**), and their cleavage to GODIC **9** and MODIC **10**.

HPLC peaks to **7** and **8** was validated by LC–MS with electrospray ionization (ESI) which shows coincidence of the diode array trace with that for the quasimolecular ion ($[M+H]^+$) of the products at m/z 543.3 and 557.3, respectively. Both compounds were isolated by preparative HPLC. The protective groups in **7**, **8** were cleaved with aqueous 3 N HCl at room temperature, and the products again purified by preparative HPLC. LC–MS measurements showed quasimolecular ions at m/z 343.2 and 357.2 for the respective compound confirming that both *t*-BOC groups in **7** and **8** have been eliminated. Accurate mass determination of the isolated products gave $[M+H]^+$ at m/z 343.2101 and 357.2256, corresponding to an elemental composition of $C_{14}H_{27}N_6O_4$ and $C_{15}H_{29}N_6O_4$, respectively. The NMR data, compiled in Table 1, unequivocally prove formation of 2-ammonio-6-({2-[(4-ammonio-5-oxido-5-oxopentyl)amino]-4,5-dihydro-1*H*-imidazol-5-ylidene}amino)hexanoate (**9**) and 2-ammonio-6-({2-[(4-ammonio-5-oxido-5-oxopentyl)-amino]-4-methyl-4,5-dihydro-1*H*-imidazol-5-ylidene}-amino)hexanoate (**10**). For these compounds, we have coined the abbreviations GODIC and MODIC, representing the terms **g**ly**o**xal- and **m**ethylgly**o**xal-**d**erived-**i**midazoline-**c**ross-link, respectively.

The NMR data sets for the heterocyclic core of MODIC **10** are more or less superimposable with those of **2**.[30] (In ref 30, the C-2 resonance of compound **8**, which is identical with compound **2** in this paper, has been erroneously given as 170.0 ppm; the correct value for δ (C-2) is 167.0 ppm.) Since the structure of **2**, especially the **exo**cyclic position of N^{δ} of the arginine moiety, has been definitely proven by $^1H, ^{13}C$ long-range correlation spectra (COLOC),[30] the close homology made it unnecessary to repeat these experiments with **10**, and to once again present the rationale by which we have arrived at this structure. Schwarzenbolz et al.[34] have identified 5-(2-amino-4-oxo-4,5-dihydro-1*H*-imidazol-3-ium-3-yl)-2-ammoniopentanoate (**11**; see Fig. 3), that is, a product with **endo**cyclic N^{δ} of the arginine side chain, from the reaction of GO with proteins. In contrast, Henle et al.[31] found 2-ammonio-5-[(4-methyl-5-oxo-4,5-dihydro-1*H*-imidazol-2-yl)amino]pentanoate (**12**) as the main product from protein–MGO incubations. Formation of **12** can be rationalized by MGO reacting directly instead of its aldimine **6**, according to the pathway given in Figure 2. To definitely prove that the GO aldimine **5** reacts analogously to **6** and does not form a product with an **endo**cyclic N^{δ} of the arginine moiety as in 6-{[2-amino-3-(4-ammonio-5-oxido-5-oxopentyl)-1,5-dihydro-4*H*-imidazol-3-ium-4-ylidene]amino}-2-ammoniohexanoate (**13**), i.e. the imine of **11**, or 6-{[2-amino-1-(4-ammonio-5-oxido-5-oxopentyl)-1,5-dihydro-4*H*-imidazol-4-ylidene]amino}-2-ammoniohexanoate (**14**), the structure of GODIC **9** was probed with a gradient-selected ^1H-detected long-range ^1H, ^{13}C-COSY (gs-HMBC) spectrum (ref 35, pp 485–488). The results are summarized in Figure 3, with the arrows indicating significant carbon–proton long-range coupling across two or three bonds (^2J or ^3J).

The gs-HMBC spectrum shows only one single cross-peak for the H_2-1″ triplet in the downfield region (i.e. with C-2). The other two cross-peaks connect this proton resonance with the non-heterosubstituted C-2″ and C-3″ of the arginine side chain. Structures **13** or **14**, in contrast, would require correlation of H_2-1″ with both quasi-carbonyl C-atoms or with the guanidine and methylene carbon, respectively, in the five-membered ring. The N^{δ} nitrogen of the L-arginine side chain thus by necessity has remained **exo**cyclic in the formation of the imidazoline ring and **9** is unequivocally established as the structure of the major product from the reaction of GO.

With the structure of the cross-links **9** and **10** definitely confirmed, an LC–ESI–MS method for their quantification was developed. To improve the retention behavior of these highly polar compounds on reversed phase

Table 1. ^1H and ^{13}C NMR data of GODIC **9** and MODIC **10** (in D_2O)[a]

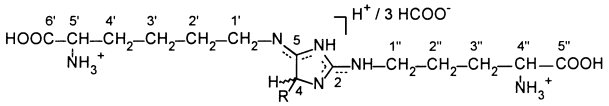

	9	**10**
R	H	CH_3
^1H NMR	δ (ppm) [b]	
H-4	—	4.72
H_2-4	4.49	—
H_3C-4	—	1.45
H_2-1′	3.43	3.43
H_2-2′	1.68	1.68
H_2-3′	1.44	1.44
H_2-4′	1.89	1.90
H-5′	3.72	3.72
H_2-1″	3.34	3.33
H_2-2″	1.69–1.75	1.69–1.75
H_2-3″	1.89	1.90
H-4″	3.76	3.76
$HCOO^-$	8.41	8.44
	J (Hz)[c]	
$^3J_{4,H_3C-4}$	—	6.9
$^3J_{1',2'}$	6.9	7.0
$^3J_{2',3'}$	7.2	7.2
$^3J_{3'4'}$	7.2	7.2
$^3J_{4',5'}$	6.1	6.1
$^3J_{1'',2''}$	6.9	6.8
$^3J_{3'',4''}$	6.1	6.1
^{13}C NMR	δ (ppm)[b]	
C-2	168.8	167.0
C-4	51.0	58.6
C-5	177.9	181.3
H_3C-4	—	18.1
C-1′	43.0	43.0
C-2′	27.8	27.8
C-3′	22.0	21.9
C-4′	30.4	30.4
C-5′	55.0	55.0
C-6′	174.8	174.7
C-1″	42.0	42.1
C-2″	24.2	24.2
C-3″	28.0	28.0
C-4″	54.7	54.7
C-5″	175.1	175.1
$HCOO^-$	170.7	171.4

[a] Hydrogen/carbon assignment has been validated by ^1H, ^1H-COSY, ^1H, ^{13}C-COSY, ^{13}C-DEPT and gs-HSQC-TOCSY measurements.
[b] δ (ppm): Chemical shift for the indicated hydrogen/carbon.
[c] *J* (Hz): Coupling constant between the indicated protons.

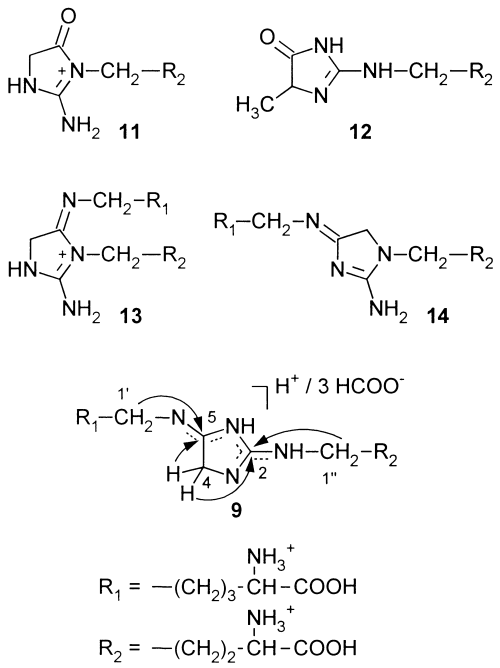

Figure 3. Structural fomulae of 5-(2-amino-4-oxo-4,5-dihydro-1*H*-imidazol-3-ium-3-yl)-2-ammoniopentanoate (**11**), 2-ammonio-5-[(4-methyl-5-oxo-4,5-dihydro-1*H*-imidazol-2-yl)amino]pentanoate (**12**), 6-{[2-amino-3-(4-ammonio-5-oxido-5-oxopentyl)-1,5-dihydro-4*H*-imidazol-3-ium-4-ylidene]amino}-2-ammoniohexanoate (**13**), 6-{[2-amino-1-(4-ammonio-5-oxido-5-oxopentyl)-1,5-dihydro-4*H*-imidazol-4-ylidene]amino}-2-ammoniohexanoate (**14**), and established structure of GODIC **9** (arrows indicating the characteristic carbon–proton long-range coupling connectivities from the gs-HMBC spectrum).

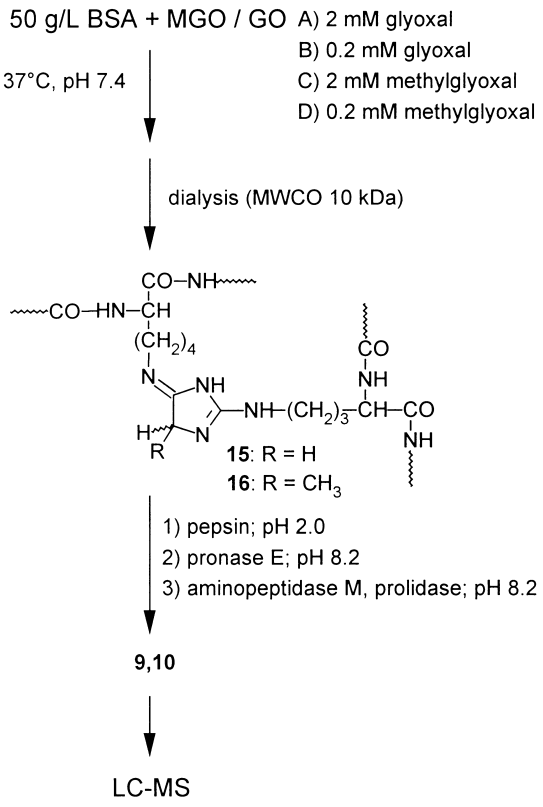

Figure 4. Schematic work up procedure for the glyoxal/methylglyoxal–BSA incubations.

(RP) material, *n*-heptafluorobutyric acid (HFBA) was added to the eluent for providing the counter ion. HFBA is widely used in HPLC analysis of peptides and proteins; since HFBA is volatile in high vacuum, it poses no problem to the MS system.

Figure 4 shows structures **9** and **10** incorporated in a protein. To prove that the cross-linking units **15** and **16** are actually formed, either intra- or intermolecularly, BSA and GO or MGO were incubated at two different concentrations (series A–D; 37°C, pH 7.4) for 1 week. Aliquots were taken after 2, 5, 22, 48, 96 and 168 h and dialyzed against water using a membrane with 10 kDa molecular weight cut-off (MWCO). Experiments with authentic synthetic material have shown that GODIC **9** and MODIC **10** both are unstable under the conditions for conventional acidic hydrolysis of proteins (6 N HCl, 110°C, 24 h). The lyophilized BSA was therefore cleaved enzymatically as described by Klostermeyer and Henle[36,37] for casein. Our own amino acid analyses have shown this procedure to be also suitable for BSA, resulting in almost quantitative hydrolysis. The hydrolyzates were diluted to avoid disturbance of the chromatography by the ion-pair activity of the tris(hydroxymethyl)aminomethane (TRIS)–HCl-buffer, employed for the enzymatic cleavage. The resulting solutions were applied to the LC–MS system operating in single-ion monitoring (SIM) mode at *m*/*z* 298.2 and 357.2, respectively. Unfortunately, GODIC **9** could not be quantified using the trace for the quasimolecular ion at *m*/*z* 343.2 due to coelution of another compound with identical $[M+H]^+$, presumably a tripeptide. This coincidence could not be resolved by changing the chromatographic conditions or the stationary phase. Therefore, a fragment ion of **9** at *m*/*z* 298.2 was used for quantification; this ion is lacking in the MS spectrum of the coeluting compound. The sensitivity for GODIC **9** thus is reduced to about one fourth.

The LC–MS system was calibrated in the range of 72.3–2312 μg **9**/L and 13.1–420 μg **10**/L, respectively. The linear calibration graphs are described by the equations area = (−2180 ± 443) + (31.66 ± 0.41) L/μg×c(**9**) and area = (−356 ± 295) + (56.61 ± 1.49) L/μg×c(**10**), the values in parenthesis representing means ± confidence intervals (p = 95%). The standard error (s_R) was determined as 280.7 and 186.6, respectively. Limits of detection (LOD) 56.4 or 20.9 μg/L, and limits of quantitation (LOQ) 146.8 or 35.2 μg/L for **9** or **10** were calculated according to the recommendations of the Deutsche Forschungsgemeinschaft (DFG).[38] The amounts of **9** and **10**, determined for the incubation series A–D, can be correlated with the derivatization rate of arginine side chains in the BSA molecule as demonstrated in Figure 5.

The concentrations found for the incubation series B and D are below the calculated LOQ. Nevertheless, Figure 5 includes values above the respective LOD, towards the end of the reaction period, to give a rough impression of the conversion rate relative to the other

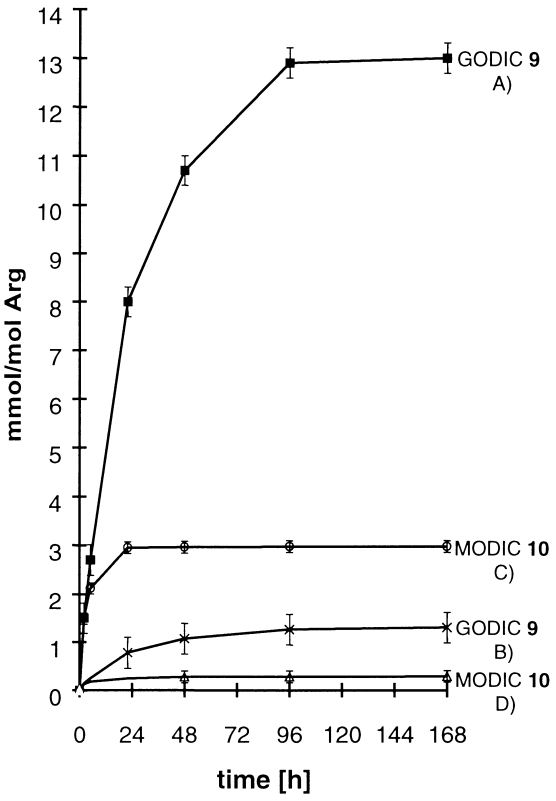

Figure 5. Time course for the formation of the cross-links **9** and **10** in the glyoxal/methylglyoxal–BSA incubations.

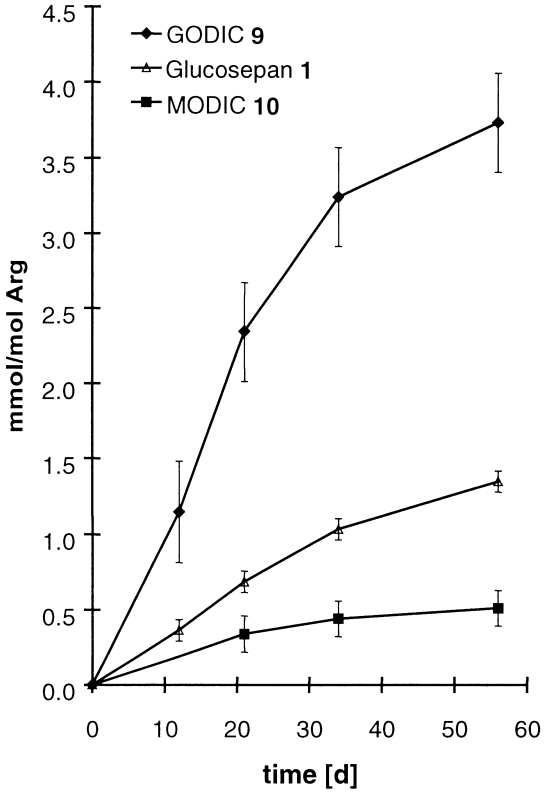

Figure 6. Time course for the formation of GODIC **9**, glucosepan **1**, and MODIC **10** in a D-glucose–BSA incubation.

two series A and C. Reducing the α-dicarbonyl concentration from 2 to 0.2 mM in both cases leads to an almost proportionally lower yield of the products **9** and **10**. Since the BSA molecule contains 23 arginine units, the maximum value of 13.0 ± 0.32 mmol **9**/mol Arg for series A, and 3.0 ± 0.12 mmol **10**/mol Arg for series C signifies that statistically about every third or 15th BSA molecule contains one of the cross-linking units **15** or **16**. The high conversion rate to GODIC **9** even allows monitoring of this compound by DAD and additional identification by its UV spectrum.

To prove that **9** and **10** are also formed with D-glucose instead of GO or MGO as substrate, we re-analyzed samples from an incubation of 100 mM D-glucose with 50 g/L BSA, which had originally been used for the quantification of glucosepan **1**.[29] The graphs for GODIC **9**, glucosepan **1**, and MODIC **10** are given in Figure 6. GODIC shows the highest formation rate with 3.7 ± 0.32 mmol **9**/mol Arg after 8 weeks incubation time, followed by glucosepan and MODIC with 1.38 ± 0.07 mmol **1**/mol Arg and 0.5 ± 0.12 mmol **10**/mol Arg, respectively.

The important role of **9** and **10** in protein cross-linking becomes even more apparent if their formation is compared with that of GOLD **3** and MOLD **4** (see Fig. 1) as a function of concentration of the respective α-dicarbonyl precursor in a model system. We have reacted 200, 20, 2 and 0.2 mM GO or MGO with 50 mM α-*N*-*t*-BOC-L-lysine and α-*N*-*t*-BOC-L-arginine for 24 h under physiological conditions, and analyzed the mixtures by LC–MS. The exact concentration of the commercially available GO and MGO solutions (~40%) was determined after reduction with sodium borohydride and quantification of the resulting ethylene glycol and 1,2-propanediol by HPLC with refractive index (RI) detection (not detailed in Experimental). The results of the MGO incubation are shown in Figure 7.

At 200 mM MGO, only traces of **8** can be detected beside the *t*-BOC derivative of **4**. Reducing the MGO concentration by a factor of 10 leads to nearly equal intensities of the signals, obtained in the SIM mode, for the respective quasimolecular ions at *m*/*z* 541.3 and 557.3. Lowering the MGO concentration still further shifts the product ratio more and more in favor of structure **8**. Figure 8 gives a double-logarithmic plot of the α-dicarbonyl concentration versus the area ratios for the peaks of the *t*-BOC derivatives of GODIC **9** relative to GOLD **3** and of MODIC **10** relative to MOLD **4**.

Formation of the imidazoline cross-link appears favored by a power of about 10 for GO relative to MGO. At 2 mM GO and MGO, the signal area for **7** is sevenfold, and that for **8** 86-fold higher than the peak area for the corresponding imidazolium compound. At 0.2 mM GO, the signal to noise ratio for the GOLD peak is below 5:1 and thus not suitable for proper quantification; this data point has therefore been omitted from the GO graph. The concentration-dependence of the ratio in which the two compared cross-links are formed is best explained by an entropy argument: generation of **3** and **4**, in contrast to that of **9** and **10**, requires 2 mol of the respective α-dicarbonyl compound.[18,19]

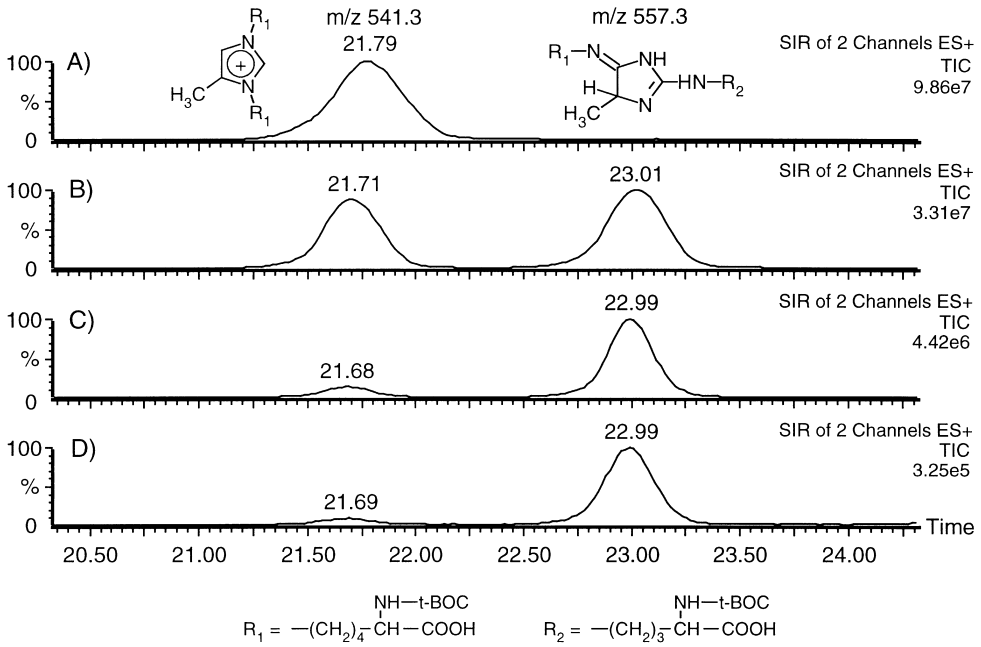

Figure 7. SIM chromatograms for the detection of MOLD **4** and MODIC **10**, at the respective $[M+H]^+$ ion mass m/z 541.3 and 557.3, in mixtures of α-*N*-*t*-BOC-L-lysine, α-*N*-*t*-BOC-Larginine, and (A) 200 mM, (B) 20 mM, (C) 2 mM, (D) 0.2 mM methylglyoxal.

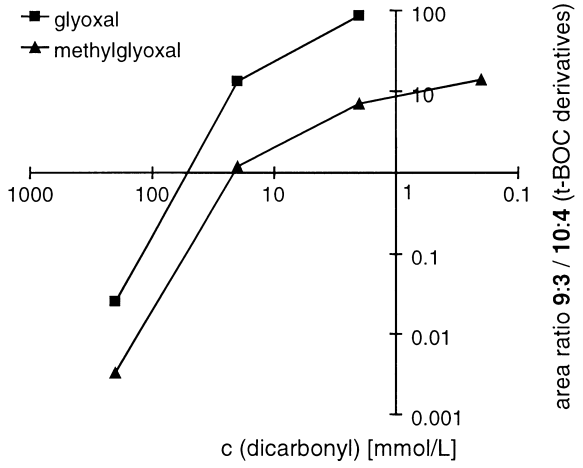

Figure 8. Double-logarithmic plot of α-dicarbonyl concentration versus area ratios for the signals of the *t*-BOC derivatives of GODIC **9** relative to GOLD **3** and MODIC **10** relative to MOLD **4**.

Discussion

Reactive dicarbonyl compounds like GO and MGO are well established as crucial intermediates in the chemical modification of proteins during degradation/oxidation of reducing sugars and autoxidation of polyunsaturated fatty acids. The majority of products have not yet been characterized. However, reaction of GO and MGO with proteins leads to formation of N^{ε}-(carboxymethyl)lysine (CML),[14,17,39] N^{ε}-(carboxyethyl)lysine (CEL),[40] and imidazolinone adducts such as **11** and **12**.[31,34] In model systems, Wells–Knecht et al. have identified the imidazolium cross-links known as glyoxal-lysine dimer (GOLD **3**) and methylglyoxal-lysine dimer (MOLD **4**; see Fig. 1).[18,19] More recently, Nagaraj et al.[28] reported the identification of **4** in human serum, and Odani et al.[41] described an ESI–MS–MS procedure for simultaneous determination of both **3** and **4** in serum proteins. Cross-linking and insolubilization are among the major biochemical changes which proteins suffer during aging. Enhancement of this process in extracellular matrix is implicated in a number of age- and diabetes-associated complications (e.g. atherosclerosis and cataract formation). Thus, in recent years, much effort has been directed towards the chemical characterization of cross-linking structures derived from the Maillard reaction.

The main target of the present study was to clarify whether and to which extent the cross-links **15** and **16** (Fig. 4) are formed in GO–BSA or MGO–BSA and D-glucose–BSA incubations under physiological conditions. The syntheses of GODIC **9** and MODIC **10** have already shown that the yield of the respective product is definitely higher with GO than with MGO. This result is mirrored by the tremendous conversion rate of GO to **15** in the BSA incubations. Under identical conditions (2 mM α-dicarbonyl compound, 50 g/L BSA, 37°C, pH 7.4), GO leads to a 4.3-fold higher cross-linking of BSA molecules than MGO by compounds **15** and **16**, as demonstrated in Figure 5. Furthermore, **15** reaches a steady state after about 4 days whereas the amount of **16** remains constant after only 1 day. This divergent reaction behavior may in part be due to the fact that MGO molecules are more prone to side reactions such as aldol condensation. The derivatization rate of 13.0 ± 0.32 mmol **9**/mol Arg implies that 11% of the GO starting material has been transformed to GODIC, and thus clearly demonstrates the potential this compound has in protein cross-linking. In the D-glucose–BSA incubation (Fig. 6), GODIC **9** likewise dominates. It must be taken into account, though, that this reaction was run without metal-complexing agents and inert gas atmosphere. Oxidation processes, essential for the formation of GO, thus are favored and contribute to the

high value for **9**. Since the biochemical origin of GO and MGO is very complex (see Introduction), the ratio of compounds **1**, **9** and **10** from the D-glucose–BSA incubation in principle cannot be extrapolated to in vivo conditions.

Figure 8 clearly shows that formation of GODIC **9** and MODIC **10** is favored at low α-dicarbonyl levels relative to that of GOLD **3** and MOLD **4**. The physiological concentration (e.g. in human blood) is 150 nM for GO (onefold increase in diabetes mellitus)[42] and 80 nM for MGO (five to sixfold increase in diabetes mellitus),[43] and thus lower by a factor of about 1000 than the lowest concentration used in our model reactions. It seems fully justified to expect, therefore, that **9** and **10** are of greater significance for the cross-linking of proteins in vivo than **3** and **4**. We are currently trying to prove this hypothesis and to quantify compounds **9** and **10**, as well as glucosepan **1**, in both human proteins and in foodstuffs.

Conclusion

The data presented above clearly demonstrate that our lysine-arginine AGEs GODIC **9**, MODIC **10** and glucosepan **1** play a decisive role in the cross-linking of proteins. It is difficult to estimate, however, whether and how much they dominate, quantitatively, in vivo over previously described compounds like pentosidine, crossline, fluorophore LM-1, GOLD **3** and MOLD **4**. This is in part due to the fact that no general procedures for suitable in vitro experiments exist which would allow comparison between the different cross-links and an at least rough extrapolation to in vivo conditions. We are presently investigating this aspect, and are trying to elaborate such a protocol.

Experimental

General methods

^{1}H NMR (500 MHz) and ^{13}C NMR (126 MHz) spectra were recorded on a Bruker (Karlsruhe, Germany) ARX 500 spectrometer in D_2O. Chemical shifts (δ) are given in ppm relative to external Me_4Si, coupling constants (*J*) in Hz. For the 2-D NMR experiments ^{1}H, ^{1}H-COSY (ref 35, pp 353–355) and ^{1}H, ^{13}C-COSY (ref 35, pp 375–377), Bruker standard software (X-WIN-NMR 2.0) was employed. For gradient-selected heteronuclear multiple bond correlation (gs-HMBC) (ref. 35, pp 485–488) and gradient-selected heteronuclear single quantum coherence total correlation spectroscopy (gs-HSQC-TOCSY) (ref 35, pp 538–541) a Varian (Darmstadt, Germany) Unity Inova 500 MHz spectrometer was used. The analytical HPLC system comprised an HP1100 autosampler, HP1100 gradient pump, HP1100 column thermoregulator, and HP1100 diode array detector (DAD) module (Hewlett Packard, Waldbronn, Germany). For data acquisition and processing, an HP Chem Station (Rev. A. 04.02) software was used. Column (YMC Europe, Schermbeck, Germany): YMC-Pack Pro C 18, 120 Å, 5 μm (guard column 10×4.6 mm, column 150×4.6 mm); column temperature 25°C; flow rate 1.0 mL/min; injection volume 20 μL; 10 mM phosphate buffer (pH 4.0)-methanol gradient: % MeOH (t (min)) 0(0)-95(30–40)-0(43–48); DAD detection wavelengths 220 and 242 nm, spectral band width (SBW) 4 nm, reference 500 nm (SBW 100 nm). LC–MS was run on an HP1100 HPLC system (modules as described above), coupled to a Micromass (Manchester, UK) VG platform II quadrupole mass spectrometer equipped with an electrospray (ESI) interface. Chromatographic conditions: column, column temperature, flow rate and injection volume were as described above; gradients: (A) 0.01 M ammonium formate buffer (pH 4.0)–MeOH, % MeOH(t (min)) 0(0)-95(30–40)-0(43–48); (B) 10 mM *n*-heptafluorobutyric acid (HFBA)–MeOH, % MeOH (t (min)) 5(0)-60(30)-95(35–40)-5(45–52); post-column splitting ratio 1:20. MS parameters: ESI+, source temperature 120°C, capillary 3.5 kV; HV lens 0.5 kV. For LC analyses the MS system was operated either in full scan mode (*m*/*z* 200–1000) or in single ion mode (SIM; span 0.5 Da, dwell time 1.0 s). For accurate mass determination,[44] data were collected in the multichannel acquisition (MCA) mode with 128 channels per *m*/*z* unit using 11 scans (5 s) with 0.1 s reset time. The resolution was 1100 (10% valley definition). The sample was dissolved for analysis in water:MeCN (1:1) containing poly(propylene glycol) 425 (0.1 μg/μL) as reference material, ammonium formate (0.1%), and formic acid (1%); the sample concentration was similar to that of PPG 425. The solution was introduced into the ESI source at a flow rate of 5 μL/min. With a *m*/*z* 305–430 scan range, five reference peaks could be used for calibration: *m*/*z* 309.2277, 326.2543, 367.2696, 384.2961, 425.3114. The preparative HPLC system consisted of a Kronlab (Sinsheim, Germany) KD200/100SS gradient pump system combined with a Knauer (Berlin, Germany) A0293 variable wavelength detector and a Kronlab HPLC column (guard column 50×20 mm, column 250×20 mm; Nucleosil C 18, 100 Å, 7 μm); flow rate 20 mL/min; ammonium formate buffer (10 mM, pH 4.0)–MeOH gradients: % MeOH (t (min)), A) 30(0)-80(17)-100(18–23)-30(24–30), B) 0(0)-10(6–10)-0(11–16); injection volume 1.0 mL; detection wavelength 242 nm. An Amicon (Witten, Germany) stirred cell 8050 equipped with an Amicon PM 10 ultrafilter was employed for dialysis. Reaction mixtures from synthetic procedures were filtered (membrane filter, 0.45 μm) before preparative HPLC. MeOH was removed from the eluent in vacuo, and the remaining aqueous layer lyophilized with a Leyboldt–Heraeus (Köln, Germany) Lyovac GT 2.

Materials

Ultrapure water, obtained from a MilliQ 185 Plus apparatus (Millipore, Eschborn, Germany), HPLC grade methanol, and HPLC grade acetonitrile were used for LC and LC–MS. For preparative HPLC solvents were degassed by flushing with helium. For a phosphate buffer salt mixture giving solutions with pH 7.4, KH_2PO_4 (2.68 g; 20 mmol) and $Na_2HPO_4{\cdot}2H_2O$ (14.30 g; 80 mmol) were mixed vigorously. α-*N*-*t*-BOC-L-Arginine, α-*N*-*t*-BOC-L-lysine, glyoxal solution (~40%), methylglyoxal solution (~40%), and prolidase

were purchased from Fluka (Neu-Ulm, Germany), *n*-heptafluorobutyric acid and poly(propylene glycol) 425 from Aldrich (Steinheim, Germany), bovine serum albumin (fraction V), diethylenetriaminepentaacetic acid, and pepsin from Sigma (Steinheim, Germany), pronase E from Merck (Darmstadt, Germany), aminopeptidase M from Boehringer Mannheim (Mannheim, Germany).

2-Ammonio-6-({2-[(4-ammonio-5-oxido-5-oxopentyl) amino]-4,5-dihydro-1*H*-imidazol-5-ylidene}amino)hexanoate (9). Glyoxal (228 μL, 2 mmol), α-*N*-*t*-BOC-L-lysine (1.23 g, 5 mmol), α-*N*-*t*-BOC-L-arginine (1.37 g, 5 mmol), and phosphate buffer pH 7.4 (0.85 g, 5 mmol) were dissolved in water (25 mL). The pH was adjusted to 7.4 with 2 N NaOH, the mixture kept at 50°C for 4 days under nitrogen, and purified by preparative HPLC (gradient A). Fractions with t_R 14.4 min yielded, after lyophilization, 47.5 mg (4.04%) 2-[(*tert*-butoxycarbonyl)amino]-6-{[2-({4-[(*tert*-butoxycarbonyl)amino]-5-oxido-5-oxopentyl}amino)-4,5-dihydro-1*H*-imidazol-5-ylidene]amino}hexanoic acid (**7**) as the respective formate; UV (H_2O): λ_{max} (nm) 242; LC–ESI–MS (gradient A): t_R 22.95 min, cone voltage (CV) 55 V, *m*/*z* 581 (5.0, $[M+K]^+$), 565 (1.4, $[M+Na]^+$), 543 (100, $[M+H]^+$), 487 (27.7), 443 (17.6), 387 (8.4), 343 (6.8).

Compound **7** (47.5 mg) was dissolved in aqueous 3 N HCl (2 mL) and kept at room temperature for 30 min. The pH was adjusted to 7 by slowly adding solid $NaHCO_3$ (160–180 mg, 1.90–2.14 mmol), the volume finally filled up to 5 mL, and the mixture purified by preparative HPLC (gradient B). Fractions with t_R 6.2 min were collected and yielded after lyophilization **9**·3 HCOOH (22.5 mg, 58%); ^1H and ^{13}C NMR (D_2O): see Table 1; UV (H_2O): λ_{max} (nm) (lg ε) 242 (4.16); LC–ESI–MS (gradient B): t_R 22.9 min, CV 50 V *m*/*z* 381 (1.3, $[M+K]^+$), 365 (5.12, $[M+Na]^+$), 343 (100, $[M+H]^+$), 298 (11.5), 280 (2.4) 228 (4.8); accurate mass (mean of eight measurements ± standard deviation): *m*/*z* 343.2101 ± 0.0004 $[M+H]^+$ (343.2094, calcd for $C_{14}H_{27}N_6O_4$).

2-Ammonio-6-({2-[(4-ammonio-5-oxido-5-oxopentyl) amino]-4-methyl-4,5-dihydro-1*H*-imidazol-5-ylidene}amino)hexanoate (10). Methylglyoxal (1.2 mL, 8.16 mmol), α-*N*-*t*-BOC-L-lysine (2.58 g, 10.5 mmol), α-*N*-*t*-BOC-L-arginine (1.94 g, 7.1 mmol) and phosphate buffer pH 7.4 (2.73 g, 16.0 mmol) were dissolved in water (12.8 mL). The pH was adjusted to 7.4 with 2 N NaOH, the mixture kept at 40°C for 24 h under nitrogen and purified by preparative HPLC (gradient A). Fractions with t_R 14.6 min yielded after lyophilization 18.9 mg (0.39%) 2-[(*tert*-butoxycarbonyl)amino]-6-{[2-({4-[(*tert*-butoxycarbonyl) amino]-5-oxido-5-oxopentyl}amino)-4-methyl-4,5-dihydro-1*H*-imidazol-5-ylidene]amino}hexanoic acid (**8**) as the respective formate; UV (H_2O): λ_{max} (nm) 242; LC–ESI–MS (gradient A): t_R 23.1 min, cone voltage (CV) 55 V, *m*/*z* 595 (2.5, $[M+K]^+$), 579 (2.8, $[M+Na]^+$), 557 (100, $[M+H]^+$), 501 (25.8), 457 (27.1), 401 (9.6), 357 (12.1).

Cleavage of the *t*-BOC groups from **8** (18.9 mg) and purification follow the procedure given above. Fractions at t_R 8.3 min were collected and yielded after lyophilization **10**·3 HCOOH (4.4 mg, 28.4%); ^1H and ^{13}C NMR (D_2O): see Table 1; UV (H_2O): λ_{max} (nm) (lg ε) 242 (4.13); LC–ESI–MS (gradient B): t_R 24.0 min, CV 50 V *m*/*z* 395 (2.8, $[M+K]^+$), 379 (4.8, $[M+Na]^+$), 357 (100, $[M+H]^+$), 312 (8.2), 294 (1.0) 242 (2.7); accurate mass (mean of nine measurements ± standard deviation): *m*/*z* 357.2256 ± 0.0008 $[M+H]^+$ (357.2250, calcd for $C_{15}H_{29}N_6O_4$).

Glyoxal/methylglyoxal–bovine serum albumin (BSA) incubations

BSA (12.5 g, 188.5 μmol) was dissolved in phosphate buffer (250 mL, 0.1 M, pH 7.4) containing diethylenetriaminepentaacetic acid (1 mM) and passed through a 0.45 μm membrane filter. To aliquots (50 mL each) of this mixture glyoxal or methylglyoxal was added: for incubation series A, 114 μL of a 1:10 dilution of the glyoxal solution (8.8 M); for incubation series B, 114 μL of a 1:100 dilution of the glyoxal solution (8.8 M); for incubation series C, 147 μL of a 1:10 dilution of the methylglyoxal solution (6.8 M); for incubation series D, 147 μL of a 1:100 dilution of the methylglyoxal solution (6.8 M). Aliquots (4×10 mL) of each series were filtered (sterile filter, 0.2 μm) into tubes, flushed with nitrogen (3 min), sealed tightly, and kept at 37°C with gentle shaking.

Work up of incubation mixtures and enzymatic cleavage of the protein

After 2, 5, 22, 48, 96 and 168 h, aliquots from all BSA incubation series (equivalent to 100 mg protein) were transferred to the Amicon stirred cell, diluted to 25 mL with water, and dialyzed with 0.8 L water by applying a pressure of 3 bar. After lyophilization, 3.5 mg of the protein obtained was cleaved enzymatically as described.[36,37] The hydrolyzates were filled up to 5 mL with water and subjected to LC–MS analysis (SIM mode). For the monitoring masses at *m*/*z* 298.2 and 357.2 cone voltages of 65 and 50 V were applied, respectively.

Formation of the imidazoline compounds 7 and 8 and the *t*-BOC derivatives of GOLD 3 and MOLD 4 as a function of the α-dicarbonyl concentration

α-*N*-*t*-BOC-L-Lysine (246 mg, 1 mmol), α-*N*-*t*-BOC-L-arginine (274 mg, 1 mmol), and phosphate buffer pH 7.4 (340 mg, 2 mmol) were dissolved in water (10 mL). To aliquots (1 mL each) glyoxal or methylglyoxal was added: 45.5 μL, (1) of the glyoxal solution (8.8 M), (2) of a 1:10, (3) of a 1:100, (4) of a 1:1000 dilution; 60 μL, (1) of the methylglyoxal solution (6.8 M), (2) of a 1:10, (3) of a 1:100, (4) of a 1:1000 dilution. The mixtures were filled up to 2 mL, flushed with nitrogen (3 min), and kept at 37°C for 24 h. The filtrates (membrane filter, 0.45 μm) were analyzed by LC–MS (SIM mode). For the monitoring masses at *m*/*z* 527.3, 543.3 and *m*/*z* 541.3, 557.3 a cone voltage of 55 V was used. Samples (1) had to be diluted 1:10 prior to injection.

Acknowledgments

We thank Priv.-Doz. Dr. P. Fischer, Institut für Organische Chemie, Universität Stuttgart, for many helpful

discussions and Professor Dr. W. Schwack, Institut für Lebensmittelchemie, Universität Hohenheim, for the excellent working conditions at his Institute. To Dr. B. Vogler, Institut für Chemie, Universität Hohenheim, J. Rebell and H.U. Höhn, Institut für Organische Chemie, Universität Stuttgart, we are grateful for the recording of the NMR spectra. For help with the statistical evaluation, thanks are due to H. van Lishaut, Institut für Lebensmittelchemie, Universität Hohenheim.

References

1. Ledl, F.; Schleicher, E. *Angew. Chem., Int. Ed. Engl.* **1990**, *29*, 565.
2. Friedman, M. *J. Agric. Food Chem.* **1996**, *44*, 631.
3. Bucala, R.; Vlassara, H.; Cerami, A. In *Post-Translational Modifications of Proteins*; Harding, J. J., Crabbe, J. C., Eds.; CRC: Boca Raton, 1992; pp 53–79.
4. Zyzak, D. V.; Wells-Knecht, K. J.; Blackledge, J. A.; Litchfield, J. E.; Wells-Knecht, M. C.; Fu, M.-X.; Thorpe, S. R.; Feather, M. S.; Baynes, J. W. In *Maillard Reactions in Chemistry, Food, and Health*; Labuza, T. B.; Reineccius, G. A.; Monnier, V. M.; O'Brien, J.; Baynes, J. W., Eds.; The Royal Society of Chemistry: Cambridge, 1994, pp 274–280.
5. Baynes, J. W.; Monnier, V. M., Eds.; *Prog. Clin. Biol. Res.*; Liss, A. R.: New York, 1989; Vol. 304.
6. Labuza, T. B.; Reineccius, G. A.; Monnier, V. M.; O'Brien, J.; Baynes, J. W., Eds. *Maillard Reactions in Chemistry, Food, and Health*; The Royal Society of Chemistry: Cambridge, 1994.
7. Cerami, A. *J. Am. Geriat. Soc.* **1985**, *33*, 626.
8. Brownlee, M. *Diabetes Care* **1992**, *15*, 1835.
9. Shin, D. B.; Hayase, F.; Kato, H. *Agric. Biol. Chem.* **1988**, *52*, 1451.
10. Richard, P. J. *Biochemistry* **1991**, *30*, 4581.
11. Phillips, S. A.; Thornalley, P. J. *Eur. J. Biochem.* **1993**, *212*, 101.
12. Loidl-Stahlhofen, A.; Spiteller, G. *Biochim. Biophys. Acta* **1994**, *1211*, 156.
13. Lo, T. W. C.; Westwood, M. E.; McLellan, A. C.; Selwood, T.; Thornalley, P. J. *J. Biol. Chem.* **1994**, *269*, 32299.
14. Wells-Knecht, K. J.; Zyzak, D. V.; Litchfield, J. E.; Thorpe, S. R.; Baynes, J. W. *Biochem.* **1995**, *34*, 3702.
15. Westwood, M. E.; Thornalley, P. J. *J. Prot. Chem.* **1995**, *14*, 359.
16. Büttner, U.; Gerum, F.; Severin, T. *Carbohydr. Res.* **1997**, *300*, 265.
17. Glomb, M. A.; Monnier, V. M. *J. Biol. Chem.* **1995**, *270*, 10017.
18. Wells-Knecht, K. J.; Brinkmann, E.; Baynes, J. W. *J. Org. Chem.* **1995**, *60*, 6246.
19. Brinkmann, E.; Wells-Knecht, K. J.; Thorpe, S. R.; Baynes, J. W. *J. Chem. Soc. Perkin Trans. 1* **1995**, 2817.
20. Vasan, S.; Kapurniotu, A.; Bernhagen, J.; Teichberg, S.; Basgen, J.; Wagle, D.; Shih, D.; Terlecky, I.; Bucala, R.; Cerami, A.; Egan, J.; Ulrich, P. *Nature* **1996**, *382*, 275.
21. Nissl, J.; Pischetsrieder, M.; Klein, E.; Severin, T. *Carbohydr. Res.* **1995**, *270*, C1.
22. Nagaraj, R. H.; Portero-Otin, M.; Monnier, V. M. *Arch. Biochem. Biophys.* **1996**, *325*, 152.
23. Kato, H.; Shin, D. B.; Hayase, F. *Agric. Biol. Chem.* **1987**, *51*, 2009.
24. Slatter, D. A.; Murray, M.; Bailey, A. J. *FEBS Lett.* **1998**, *421*, 180.
25. Monnier, V. M.; Sell, D. R. *J. Biol. Chem.* **1989**, *264*, 21597.
26. Nagaraj, R. H.; Monnier, V. M. *Biochim. Biophys. Acta* **1992**, *1116*, 34.
27. Obayashi, H.; Nakano, K.; Shigeta, H.; Yamaguchi, M.; Yoshimori, K.; Fukui, M.; Fujii, M.; Kitagawa, Y.; Nakamura, N.; Nakamura, K.; Nakazawa, Y.; Ienaga, K.; Ohta, M.; Nishimura, M.; Fukui, I.; Kondo, M. *Biochem. Biophys. Res. Commun.* **1996**, *226*, 37.
28. Nagaraj, R. H.; Shipanova, I. N.; Faust, F. M. *J. Biol. Chem.* **1996**, *271*, 19338.
29. Lederer, M. O.; Bühler, H. P. *Bioorg. Med. Chem.* **1999**, *7*, 1081–1088.
30. Lederer, M. O.; Gerum, F.; Severin, T. *Bioorg. Med. Chem.* **1998**, *6*, 993.
31. Henle, T.; Walter, A. W.; Haeßner, R.; Klostermeyer, H. *Z. Lebensm. Unters. Forsch.* **1994**, *199*, 55.
32. Sopio, R.; Lederer, M. *Z. Lebensm. Unters. Forsch.* **1995**, *201*, 381.
33. Hayase, F.; Koyama, T.; Konishi, Y. *J. Agric. Food Chem.* **1997**, *45*, 1137.
34. Schwarzenbolz, U.; Henle, T.; Haeßner, R.; Klostermeyer, H. *Z. Lebensm. Unters. Forsch.* **1997**, *205*, 121.
35. Braun, S.; Kalinowski, H.-O.; Berger, S. *150 and More Basic NMR Experiments: A Practical Course*; Wiley–VCH: Weinheim, 2nd Ed., 1998.
36. Henle, T.; Walter, H.; Klostermeyer, H. *Z. Lebensm. Unters. Forsch.* **1991**, *193*, 119.
37. Schmitz, I.; Zahn, H.; Klostermeyer, H.; Rabbel, K.; Watanabe, K. *Z. Lebensm. Unters. Forsch.* **1976**, *160*, 377.
38. Walter, H.-F.; Holtz, K.-H.; Frehse, H.; Gorbach, S. G.; Thier, H.-P. In *Rückstandsanalytik von Pflanzenschutzmitteln—Mitteilung VI der Senatskommission für Pflanzenschutz-, Pflanzenbehandlungs-, und Vorratsschutzmittel—Methodensammlung der Arbeitsgruppe 'Analytik'*; Senatskommission der Deutschen Forschungsgemeinschaft, Ed.; VCH–Verlag: Weinheim, 1991; pp 1–22 (chapter XI-A).
39. Fu, M. X.; Requena, J. R.; Jenkins, A. J.; Lyons, T. J.; Baynes, J. W.; Thorpe, S. R. *J. Biol. Chem.* **1996**, *271*, 9982.
40. Ahmed, M. U.; Brinkmann-Frye, E.; Degenhardt, T. P.; Thorpe, S. R.; Baynes, J. W. *Biochem. J.* **1997**, *324*, 565.
41. Odani, H.; Shinzato, T.; Usami, J.; Matsumoto, Y.; Brinkmann-Frye, E.; Baynes, J. W.; Maeda, K. *FEBS Lett.* **1998**, *427*, 381.
42. Thornally, P. J.; McLellan, A. C.; Lo, T. W. C.; Benn, J.; Sonksen, P. H. *Diabetes* **1996**, 45(Suppl. 2), 230A.
43. McLellan, A. C.; Thornalley, P. J.; Benn, J.; Sonksen, P. H. *Clin. Sci.* **1994**, *87*, 21.
44. Tyler, A. N.; Clayton, E.; Green, B. N. *Anal. Chem.* **1996**, *68*, 3561.